Differential Effects on N_2 Binding and Reduction, HD Formation, and Azide Reduction with α-195^{His}- and α-191^{Gln}-Substituted MoFe Proteins of *Azotobacter vinelandii* Nitrogenase†

Karl Fisher, Michael J. Dilworth,‡ and William E. Newton*

Department of Biochemistry, The Virginia Polytechnic Institute and State University, Blacksburg, Virginia 24061

Received July 31, 2000; Revised Manuscript Received October 10, 2000

ABSTRACT: In contrast to the wild-type MoFe protein, neither the α-195^{Asn} nor the α-191^{Lys} MoFe protein catalyzed N_2 reduction to NH_3, when complemented with wild-type Fe protein. However, N_2 was bound by the α-195^{Asn} MoFe protein and inhibited the reduction of both protons and C_2H_2. The α-191^{Lys} MoFe protein did not interact with N_2. With the α-195^{Asn} MoFe protein, the N_2-induced inhibition of substrate reduction was reversed by removing the N_2. Surprisingly, even though added H_2 also relieved N_2 inhibition of substrate reduction, the α-195^{Asn} MoFe protein did not catalyze HD formation under a N_2/D_2 atmosphere. This observation is the first indication that these two reactions have different chemical origins, prompting a revision of the current hypothesis that these two reactions are consequences of the same nitrogenase chemistry. A rationale that accounts for the dichotomy of the two reactions is presented. The two altered MoFe proteins also responded quite differently to azide. It was a poor substrate for both but, in addition, azide was an electron-flux inhibitor with the 195^{Asn} MoFe protein. The observed reactivity changes are correlated with likely structural changes caused by the amino acid substitutions and provide important details about the interaction(s) of N_2, H_2, D_2, and azide with Mo-nitrogenase.

Like all molybdenum-dependent nitrogenases, the *Azotobacter vinelandii* enzyme is composed of two metalloproteins, the MoFe protein[1] and the Fe protein (*1*), each of which is named to reflect its metal composition. The three-dimensional crystal structures of both the isolated and complexed MoFe protein (*2*−*5*) have defined both the disposition of the elements comprising the two types of prosthetic groups accommodated within the nitrogenase MoFe protein and their bonding to the surrounding polypeptide matrix. The $\alpha_2\beta_2$ MoFe protein may be considered as a dimer of dimers with each α/β-subunit pair containing one example of both types of prosthetic group. The first type, the FeMo-cofactor (*6*), has the composition Mo-Fe7-S9-homocitrate, and contains the site(s) that bind(s) substrates and inhibitors (*7, 8*). The second prosthetic group type is the P cluster, which has the composition Fe8-S7. When dithionite is used as the reductant (*9*), the P cluster receives electrons apparently one-at-a-time from the smaller Fe protein component of nitrogenase (*10*−*13*) and forwards them to the substrate via the FeMo-cofactor. Each Fe protein−MoFe protein association and electron-transfer event involves hydrolysis of approximately two molecules of MgATP. A mandatory dissociation of the two component proteins then occurs to allow the now oxidized Fe protein to be rereduced and to exchange the spent nucleotide in order to re-enter the catalytic cycle (*14, 15*).

Both component proteins, a source of suitable reducing power (sodium dithionite in vitro), MgATP, and an anaerobic environment are essential for substrate reduction, but just how substrates interact with the FeMo-cofactor center remains undefined. However, a detailed scheme that accounts for nitrogenase kinetics has been described (*15*). This scheme is based on cycles of association and dissociation of the two wild-type nitrogenase proteins as described above. A number of these electron-transfer cycles must be completed in order to reduce substrate because no substrate is reduced to product in a single electron-transfer event. Thus, the MoFe protein is hypothesized to accumulate increasing numbers of electrons and to assume different, increasingly reduced, redox states. These redox states are labeled [E_n], where *n* is the number of electrons that have been accepted relative to the resting state ([E_0]) of the MoFe protein as prepared in the presence of dithionite. Each electron accepted by the MoFe protein is accompanied by a proton. The scheme demands that reduced MoFe protein must dissociate from the Fe protein before it can bind substrate and release product (*16*). Although these various reduced MoFe protein species are invoked by the scheme during turnover, most of them have been characterized only by the kinetics of product formation.

Under conditions of very low electron flux, i.e., with a 1:100 Fe protein:MoFe protein molar ratio, the single-

† Support from the National Institutes of Health (Grant DK37255 to W.E.N.) is gratefully acknowledged.

* Correspondence should be addressed to this author. Tel: (540) 231-8431; Fax: (540) 231-9070; E-mail: wenewton@vt.edu.

‡ Permanent address: Center for *Rhizobium* Studies, School of Biological Sciences and Biotechnology, Division of Science, Murdoch University, Murdoch, Western Australia 6150.

[1] Abbreviations: MoFe protein, molybdenum- and iron-containing protein of nitrogenase; Fe protein, iron-containing protein of nitrogenase; FeMo-cofactor, molybdenum- and iron-containing prosthetic group of the MoFe protein; EDTA-Na_2, disodium salt of ethylenediaminetetraacetic acid; EPR, electron paramagnetic resonance spectroscopy; HEPES, *N*-(2-hydroxyethyl)piperazine-*N*′-2-ethanesulfonic acid; MgATP, magnesium salt of adenosine triphosphate; PCR, polymerase chain reaction; SDS−PAGE, sodium dodecyl sulfate−polyacrylamide gel electrophoresis.

10.1021/bi0017834 CCC: $19.00
Published on Web 11/23/2000

electron-reduced MoFe protein species ([E_1]) accumulates until the concentrations of [E_0] and [E_1] are essentially equal, whereas any two-electron-reduced species ([E_2]) that is formed reverts to [E_0] by evolving H_2 (*17*). At high electron flux, e.g., at a 20:1 Fe protein:MoFe protein molar ratio, H_2 is evolved from the three- and four-electron-reduced MoFe protein species, [E_3] and [E_4], respectively. Acetylene binds reversibly to both [E_1] and [E_2], and C_2H_4 is released after a total of three electron transfers have occurred to regenerate [E_1] (*18*).

When N_2 is present, it binds reversibly to [E_3] (or to [E_4]) and displaces H_2 when doing so to produce [$E_3-(N_2)$] (or [$E_4-(N_2)$]) (*15*). This reversible interaction also forms the scheme's basis for explaining the ability of H_2 to inhibit competitively N_2 reduction to NH_3 because H_2 can, in its turn, displace N_2 (see reaction 1 below). Alternatively, the resulting bound hydrides may be protonated to produce H_2. N_2 is the only nitrogenase substrate whose reduction is inhibited by H_2 (*19*−*22*). A second feature of H_2/N_2 interactions is the nitrogenase-catalyzed formation of HD in the presence of N_2 and D_2 (*22*−*29*). HD formation is not a simple D_2:H_2O exchange process but has all the requirements of a nitrogenase-dependent reaction. With wild-type nitrogenase under N_2/D_2, electrons appearing as HD (one electron is required for each HD formed; *22, 30*) are diverted exclusively from NH_3 formation and, therefore, concomitant H_2 evolution is unaffected. The scheme explains HD formation by D_2 displacing N_2 reversibly from the [$E_3-(N_2)$] intermediate to give bound deuterides (*16, 31*). The deuterides can then be protonated to produce HD and regenerate [E_1], which can then re-enter the catalytic cycle (see reaction 2).

H_2 Inhibition of N_2 Binding:

$$[E_3-(N_2)] \underset{+N_2/-H_2}{\overset{+H_2/-N_2}{\rightleftharpoons}} [E_3-H_2] + H^+ \rightarrow [E_1-H] + H_2 \quad (1)$$

HD Formation under D_2/N_2:

$$[E_3-(N_2)] \underset{+N_2/-D_2}{\overset{+D_2/-N_2}{\rightleftharpoons}} [E_3-D_2] + H^+ \rightarrow [E_1-D] + HD \quad (2)$$

These similarities are the basis for the suggestions that HD formation under D_2/N_2 and H_2 inhibition of the N_2-to-NH_3 reaction are different manifestations of the same nitrogenase chemistry, where E represents the binding site on the enzyme. Other models of these phenomena have been described (*22, 23, 25, 28, 32*), some of which invoke reduced N−N species as the HD-forming entity.

We have been investigating the effects of substituting various amino acid residues in the FeMo-cofactor environment (see Figure 1) on the catalytic capability of the resulting altered nitrogenases (*8, 33*−*36*). More recently, we have concentrated on results of the substitutions at the α-191^{Gln} and α-195^{His} residues of the MoFe protein (*29, 37, 38*). When the α-195^{His} residue was replaced with glutamine, the resulting altered MoFe protein, which is abbreviated as α-195^{Gln} MoFe protein, resembled wild type in its interactions with H^+, acetylene, and CO, but only poorly catalyzed the reduction of both N_2 and azide (*29, 34*). In fact, both N_2 and azide acted primarily as reversible inhibitors of electron flux. In contrast, the α-191^{Gln}-substituted MoFe proteins were relatively ineffective C_2H_2 reducers with H_2-evolution activities

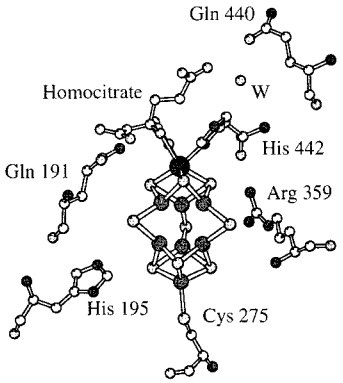

FIGURE 1: FeMo-cofactor environment of the wild-type nitrogenase MoFe protein (*2, 3*). The two residues, α-191^{Gln} and α-195^{His}, which were substituted in this work are shown on the left. Homocitrate (top left) provides two bonds to the Mo atom and is involved in putative −NH→O− hydrogen bonds with the amide functions of both α-191^{Gln} and α-440^{Gln}. The ϵ-N of the imidazole ring of α-195^{His} forms a putative −NH→S− hydrogen bond to one of the three sulfides, which hold the two subclusters of the FeMo-cofactor together. The Mo atom of the FeMo-cofactor is the largest black sphere; the Fe atoms are smaller dark gray spheres; and the S atoms are the smaller lighter-colored gray spheres. The smallest spheres represent the following: C atoms, uncolored; O atoms, gray; and N atoms, black. The figure was drawn using MOLSCRIPT (*53*).

that were inhibited by added CO (*33, 37*). No data are available for any α-191^{Gln}-substituted MoFe protein concerning either the reduction of azide or its inhibition of electron flux.

In this report, we use the wild-type, α-195^{Asn}, and α-191^{Lys} MoFe proteins to gain insight into the interaction of nitrogenase with N_2. Our first goal was to determine if N_2 inhibited substrate reduction, particularly of either protons or C_2H_2, catalyzed by either the α-195^{Asn} or the α-191^{Lys} MoFe protein, even though N_2 is not reduced to NH_3 by either nitrogenase. Second, if inhibition occurred, could it be reversed by either removing the added N_2 or adding H_2? Third, if either altered MoFe protein showed that added H_2 relieved N_2 inhibition of substrate reduction, would it also produce HD when D_2 was used in place of H_2? Fourth, because N_2 is a product of nitrogenase-catalyzed azide reduction (*29, 39*−*41*), we sought additional mechanistic insight into the functioning of Mo-nitrogenase through its interaction(s) with both HN_3 and N_3^-. Here, we show that the α-195^{Asn} and α-191^{Lys} MoFe proteins respond quite differently from one another and from both wild-type and α-195^{Gln} MoFe proteins and, in doing so, provide important details about the interaction(s) of N_2, H_2, and D_2 with nitrogenase.

EXPERIMENTAL PROCEDURES

Cell Growth and Protein Purification. The growth of wild-type (α-191^{Gln}/α-195^{His}), DJ255 (α-191^{Lys}/α-195^{His}), and DJ178 (α-191^{Gln}/α-195^{Asn}) strains of *Azotobacter vinelandii*, nitrogenase derepression, cell extract preparation, purification of the nitrogenase MoFe protein component, and exchange into 25 mM HEPES (pH 7.4) were performed as previously described (*33, 34, 37*). The resulting specific activities are listed in Table 1. The Fe protein fraction was purified to a specific activity of 2800 nmol of H_2 produced·(min·mg)$^{-1}$. The method of Lowry et al. (*42*) was used for protein concentration determinations, and SDS−PAGE with Coomassie Blue staining was used to determine the state of homogeneity of all proteins. All buffers were saturated with

Table 1: Product Formation and ATP/2e$^-$ Ratio for Proton and Azide Reduction with MoFe Proteins from Wild-Type and Mutant Strains

MoFe protein	conditions[a] and products[b]						
	argon		argon + 10 mM NaN_3				
	H_2	ATP/2e$^-$ [c]	H_2	N_2	N_2H_4	NH_3	ATP/2e$^-$ [c]
wild type	2600	4.5	1300	630	160	880	5.3
α-195^{Gln} [d]	2700	4.8	750	47	9	83	24
α-195^{Asn}	1500	4.6	1000	ND[e]	14	100	6.2
α-191^{Lys}	1500	5.7	1300	ND[e]	26	100	6.0

[a] Normal assay conditions under 101 kPa Ar with a 20-fold molar excess of wild-type Fe protein in either the absence or the presence of 10 mM sodium azide. [b] Product formation is expressed as specific activity in nmol·[min·(mg of MoFe protein)]$^{-1}$ of each product. Data are reported to two significant figures. [c] Expressed as the number of MgATP molecules hydrolyzed for each electron pair found in all measured products. [d] All data for the α-195^{Gln} MoFe protein are taken from the literature (*29*). [e] ND, not determined, but see Discussion.

argon and contained 2 mM sodium dithionite. Metal content was measured by inductively coupled plasma atomic emission spectroscopy on a Perkin-Elmer Plasma 400 spectrometer. Their molybdenum content (0.9 vs 1.9 Mo atoms per molecule for the wild type), but not their iron-to-molybdenum ratio [(13−14):1 for all MoFe proteins], indicates that both the α-195^{Asn} and α-191^{Lys} MoFe protein preparations are mixtures of approximately equal amounts of holo- and apo-MoFe protein.

PCR and DNA Sequencing. Whole cells were diluted in sterile water and lysed by heating at 100 °C for 30 min. PCR was used to amplify the region of the MoFe protein α-subunit containing the α-subunit residue of interest using oligonucleotides Fp1 (CGTAACAAGCACCTGGCC, sense) and Rp1 (GAGCATGACGCGCTTGCC, antisense). The primers were synthesized by DNAgency (Malvern, PA). PCR was performed in a MJ Research PT-100 thermocycler. Reaction conditions were initial denaturation at 94 °C for 5 min, followed by 36 cycles of denaturation at 94 °C for 30 s, annealing at 55 °C for 30 s, and extension at 72 °C for 1 min, and then a final extension at 72 °C for 5 min. The amplified products were electrophoresed through a 1% agarose gel and visualized by ethidium bromide staining. The 1 kb DNA fragment of interest was excised from the gel and purified using a silica matrix agarose gel DNA extraction kit (Boehringer Mannheim, Indianapolis, IN).

Automated DNA sequencing was performed in Virginia Tech's DNA Sequencing Facility using standard methods on an ABI 377 Automated DNA Sequencer and using PE Biosystems Big Dye Terminator chemistry. Cycle sequencing reactions were performed using 10 ng/100 bp of PCR product and PE Biosystems Big Dye Terminator ready reaction kit (Foster City, CA). Primer (Rp1, Fp1) amounts in the reaction were 3.2 pmol, and the total reaction volume was 15 μL. Cycling parameters were 25 cycles of 30 s at 95 °C, 15 s at 50 °C, and 4 min at 60 °C. Samples were then refrigerated until used. Reactions were purified using Millipore Multiscreen plates, and then dried and resuspended as per manufacturer's protocols for loading on the ABI 377 automated sequencer. Sequences were viewed using the Chromas 1.56 software.

Nitrogenase Assays. Unless otherwise stated, assays were performed at a total protein concentration of 0.5 mg·mL^{-1} with a 20-fold molar ratio of wild-type Fe protein over either wild-type or altered MoFe protein at 30 °C in 9.25 mL reaction vials fitted with butyl rubber stoppers and crimped with aluminum caps. Each assay contained, in a reaction volume of 1 mL, 30 μmol of creatine phosphate, 25 μmol of HEPES buffer (pH 7.4), 20 μmol of sodium dithionite, 5 μmol of $MgCl_2$, 2.5 μmol of ATP, and 0.125 mg (25 units) of creatine phosphokinase. Gaseous substrates and/or inhibitors were added by a gastight syringe to an atmosphere of either 101 kPa argon or 101 kPa N_2 and the vials then vented to atmospheric pressure. After a 3 min incubation period at 30 °C, the reaction was initiated by addition of premixed nitrogenase components. All assays were terminated, usually after 22 min, by injection of 0.25 mL of 0.5 M EDTA-Na_2 (pH 7.5). Assays were run at least in duplicate and most often in triplicate.

Assays under Hyperbaric pN_2. These experiments were performed under the same conditions and in the same vials, which contained 0.05 mL of 10% (v/v) C_2H_4 as a marker gas. The appropriate additional volume of N_2, e.g., 8 mL of N_2 to give 202 kPa, was injected immediately after protein addition. Such assays were terminated after 15 min and then vented to ambient pressure before gas samples were analyzed for H_2. The recovery of C_2H_4 was used to correct for the proportion of H_2 lost by venting.

Inhibition of C_2H_2 Reduction by Added N_2. These experiments were performed in the same vials to which 0.3−2.5 kPa of C_2H_2 was added to either 101 kPa Ar or 101 kPa N_2. The reactions were run for 15 min and then terminated.

Assays to determine the reversibility of the inhibition of C_2H_2 reduction by N_2 were conducted under 1 kPa C_2H_2 in either 100 kPa Ar or 100 kPa N_2 for 14 min, and C_2H_4 and C_2H_6 production was quantified every 2 min. A third assay under 1 kPa C_2H_2/100 kPa N_2 was run and C_2H_4 and C_2H_6 production quantified for 4 min, at which time the assay vial was rapidly evacuated and refilled with 1 kPa C_2H_2/100 kPa Ar and the experiment was continued for 10 min more. Effective removal of N_2 was monitored by gas chromatography.

To determine the effect of H_2 on the N_2 inhibition of C_2H_2 reduction, assays containing 1 kPa C_2H_2 in 100 kPa Ar, 100 kPa N_2, 100 kPa Ar/101 kPa H_2, or 100 kPa N_2/101 kPa H_2 were run for 22 min at 30 °C. Assays were vented to atmospheric pressure and terminated with 0.25 mL of 0.5 M EDTA-Na_2 (pH 7.5) before H_2, C_2H_4, and C_2H_6 production was quantified.

HD Formation. A series of round-bottom flasks of about 14 mL capacity, each with a ground-glass tap assembly capped by a rubber septum, were evacuated and then filled with either Ar or N_2, after addition of the reaction components. All flasks were equilibrated at 30 °C for 3 min, and vented. Fifty percent of the atmosphere was removed and replaced by 6.5 mL of D_2. Those flasks under 51 kPa D_2/50 kPa N_2 were then spiked with 0.2 mL of Ar as an internal mass-spectrometric standard. Except for the control flasks, which were used to measure background levels of H_2 and HD, the reactions were initiated by addition of premixed nitrogenase component proteins. All assays were terminated after 20 min by injection of 0.50 mL of 0.5 M EDTA-Na_2 (pH 7.5). The liquid contents were then frozen by immersion in a dry ice−ethanol bath before the contents of the atmosphere were quantified by mass spectrometry.

Catalyzed Azide Reduction. The experiment vials contained 10 mM sodium azide, and the assays were performed as described above. After termination, a 0.2 mL aliquot of the atmosphere was removed for H_2 quantification. A 0.8 mL aliquot of the liquid contents was added directly to 1.2 mL of a *p*-dimethylaminobenzaldehyde solution and the resulting absorbance read at 458 nm to quantify hydrazine production (*39*). A separate 1 mL aliquot of the liquid contents was then applied to a 2.5 cm × 6 mm Dowex-1X2 (Cl^- form) column and washed through with 2 × 0.5 mL portions of water, and samples of the effluent were analyzed for creatine (*43*). A 1.7 mL aliquot of this effluent was then applied to a 1.5 cm × 6 mm column of Dowex-50X8 (Na^+ form) and washed with 2 × 0.5 mL of water and 2 × 0.5 mL of 0.25 M NaCl. Ammonia was then eluted with four 0.5 mL volumes of 2 M NaCl and quantified by the indophenol method (*44*).

Analytical Methods. Dihydrogen evolution was measured by gas chromatography on a molecular sieve 5A column (Supelco, Bellefonte, PA) and a TC detector. Ethylene and ethane were quantified with a Porapak N column and FID detection. The calibration gases used were 1000 ppm of C_2H_4 in He, 1000 ppm of C_2H_6 in He, and 1% H_2 in N_2 (Scott Specialty Gases, Inc., Plumsteadville, PA). Creatine, as a measure of MgATP hydrolysis, was determined by the method of Ennor (*45*). NH_3 was measured on an aliquot of this effluent by the phenol−hypochlorite method after adsorption and elution from a 1.5 cm × 6 mm column of Dowex-50W-X8 (Na^+ form) to remove creatine, which interferes with the color development (*44*).

Dihydrogen (H_2) and HD produced in incubations under deuterium (D_2) were measured mass spectrometrically as the mass 2 and 3 peaks, respectively, on a model 7070 E-HF mass spectrometer (VG Analytical, Manchester, U.K.). The standards used were either added internal argon or directly by reference to D_2 after determination of the relative ionization efficiencies for H_2, D_2, and Ar. For HD, an ionization efficiency intermediate between H_2 and D_2 was assumed.

RESULTS

DNA Sequencing. By careful control of both the growth and isolation protocols, we were able to purify each of the altered MoFe proteins to very high specific activity. To ensure that we did indeed have the correct mutant strain carrying the desired altered MoFe protein, we confirmed not only the phenotype (e.g., the distribution of electron flux among concomitantly evolved products) but also the genotype. In all strains tested, DNA sequencing of both strands confirmed that the original mutation was still in place.

Effect of pN_2 on the Inhibition of H_2 Evolution and on the ATP/2e$^-$ Ratio. Unlike the α-195^{Gln} MoFe protein, which is capable of very poor but measurable N_2 fixation (*29*), the α-195^{Asn} MoFe protein is totally incapable of reducing N_2, consistent with an earlier report (*8*). However, its rate of H_2 evolution of 1260 nmol (min·mg)$^{-1}$ under 101 kPa argon is inhibited significantly when the argon is replaced by 101 kPa N_2. In addition, the N_2 atmosphere uncouples MgATP hydrolysis from electron transfer to product, resulting in an increased ATP/2e$^-$ ratio compared to the situation under argon. Figure 2 shows that inhibition of total electron flux is at a maximum (about 30%) at 101 kPa N_2. Half-maximum inhibition occurs at about 30 kPa N_2. Simultaneously, the ATP/2e$^-$ ratio increases from 4.7 under 101 kPa argon to 7.2 under 101 kPa N_2 and further to 8.2 at 202 kPa N_2. With the α-191^{Lys} MoFe protein, the rate of H_2 evolution of 1520 nmol (min·mg)$^{-1}$ under 101 kPa argon was unaffected by replacement with 101 kPa N_2, which produced a rate of 1500 nmol of H_2 (min·mg)$^{-1}$. The ATP/2e$^-$ ratio was similarly unaffected and remained at 5.8 ± 0.3.

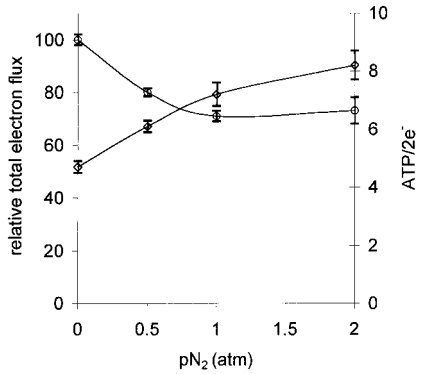

FIGURE 2: Inhibition of H_2 evolution (○) by increasing concentrations of N_2 and its effect on the ATP/2e$^-$ ratio (◇) with the α-195^{Asn} MoFe protein. At pN_2 below 1 atm (101 kPa), the balance gas was argon to 1 atm.

C_2H_2 Reduction and Effect of Added N_2. With the α-195^{Asn} MoFe protein, the rates of both C_2H_4 and C_2H_6 production were inhibited by 28% when 2 kPa C_2H_2/99 kPa N_2 replaced 2 kPa C_2H_2/99 kPa Ar. The pressure of C_2H_2 used in similar experiments with the α-191^{Lys} MoFe protein was higher. It ranged from 2 to 10 kPa in either Ar or N_2, because the K_m for C_2H_2 reduction for the α-191^{Lys} MoFe protein is 35 kPa (*37*), which is 70 times higher than that for the α-195^{Asn} MoFe protein. Even so, N_2 inhibited neither the very moderate rates of C_2H_4 and C_2H_6 production nor the rate of H_2 evolution. The ATP/2e$^-$ ratio was also unaffected and remained at 5.0 ± 0.4.

The nature of the inhibition by N_2 of C_2H_2 reduction catalyzed by the α-195^{Asn} MoFe protein was investigated by varying the pC_2H_2 between 0.3 and 2.5 kPa in an atmosphere of either Ar or N_2. Figure 3 shows that the measured K_m for C_2H_2 reduction to C_2H_4 increased from 1.0 kPa in Ar to 2.7 kPa in N_2. Identical results were obtained for C_2H_2 reduction to C_2H_6 (data not shown). The pattern produced by the two lines indicates that N_2 is a "competitive" inhibitor of C_2H_2 reduction as found previously for the nitrogenases containing either the wild-type or the α-195^{Gln} MoFe protein (*34*, *46*; but see *47*).

The reversibility of the inhibition of C_2H_2 reduction by N_2 with the α-195^{Asn} MoFe protein was tested in assays in which the initial 1 kPa C_2H_2/100 kPa N_2 atmosphere was switched after 4 min to a 1 kPa C_2H_2/100 kPa Ar atmosphere. The rates of C_2H_4 and C_2H_6 production were quantified during both stages of the experiment. These rates were compared with those obtained from undisturbed assays under either atmosphere. Figure 4 shows the inhibitory effect of N_2 on C_2H_4 production and the result of switching the atmosphere to C_2H_2 in Ar. An identical effect was observed on C_2H_6 production (data not shown). In both cases, N_2 inhibited product formation by ca. 40%. When Ar was introduced to displace the N_2, the rates of C_2H_4 and C_2H_6 production recovered to 90% of those originally measured under Ar.

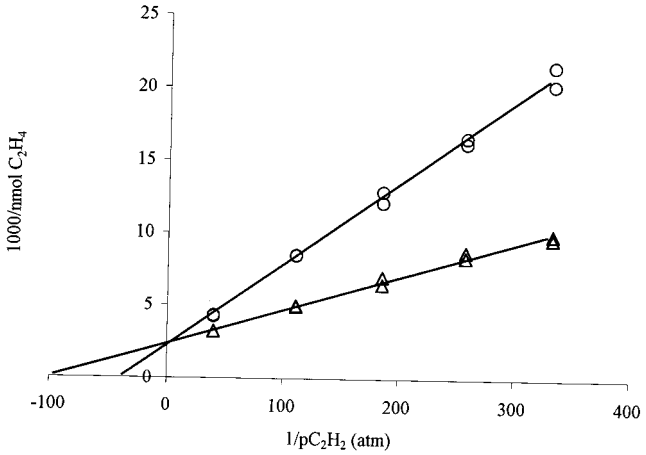

FIGURE 3: Competitive nature of N_2 as an inhibitor of C_2H_2 reduction by the α-195^{Asn} MoFe protein. The Lineweaver−Burk plots present C_2H_2 reduction as a function of C_2H_2 concentration, which ranged between 0.3 and 2.5 kPa, with either Ar (△) or N_2 (○) as the balance gas. Each line was fitted independently by linear regression. The K_m for C_2H_2 reduction was calculated as 1 kPa under Ar (in agreement with ref *37*) and 2.7 kPa under N_2.

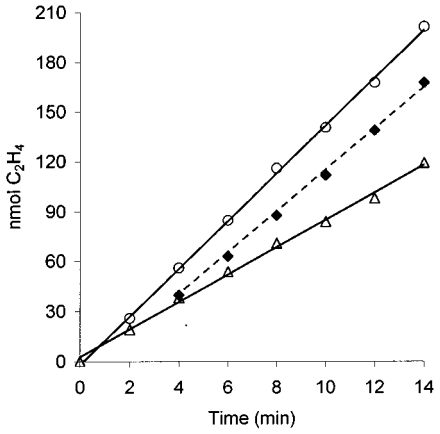

FIGURE 4: Reversibility of the inhibition by N_2 of C_2H_2 reduction by the α-195^{Asn} MoFe protein. Time courses are shown for assays containing 1 kPa C_2H_2 with either 100 kPa Ar (○) or 100 kPa N_2 (△). A third time course was run under 1 kPa C_2H_2/100 kPa N_2, and, after 4 min, this atmosphere was substituted by an atmosphere of 1 kPa C_2H_2/100 kPa Ar (◆) and the assay continued to completion. The amount of C_2H_4 present at 4 min was added to that produced at each subsequent time point, and this sum was plotted in the figure. All lines were fitted independently by linear regression.

Product Formation under Mixed H_2/N_2 or D_2/N_2 Atmospheres. Additional assays were conducted in the presence of an additional 101 kPa H_2. Figure 5 shows that, when 1 kPa C_2H_2 was used, 100 kPa N_2 inhibited the rates of both C_2H_4 and C_2H_6 production by ca. 40%. When 101 kPa H_2 was also present, these rates recovered to 95% (or better) of the respective uninhibited rates, indicating that H_2 completely reverses the N_2-induced inhibition of C_2H_2 reduction.

The rate of H_2 evolution by the α-195^{Asn} MoFe protein under 51 kPa D_2/50 kPa N_2 was 97% of that under 51 kPa D_2/50 kPa Ar. H_2 was the only product under either atmosphere with no detectable N_2-catalyzed HD formation.

Catalyzed Azide Reduction. Azide is used as a collective descriptor for all species in NaN_3 solutions, whereas the chemical formulas, either N_3^- or HN_3, are used to refer to the individual species present. Table 1 shows that, as found for the α-195^{Gln} MoFe protein (*29*), azide was a poor substrate for both the α-191^{Lys} and α-195^{Asn} MoFe proteins. The α-195^{Asn} and α-191^{Lys} MoFe proteins have higher rates (ca. 1.4-fold) of production for both N_2H_4 and NH_3 than those found for the α-195^{Gln} MoFe protein, but they are still only ca. 10% of the wild-type rates. Azide reduction to both N_2H_4 and NH_3 catalyzed by the α-195^{Asn} MoFe protein was completely eliminated by the addition of 10 kPa CO, which also reversed the electron-flux inhibition caused by azide (data not shown). In contrast, 101 kPa H_2 had no effect on either substrate reduction or electron-flux inhibition (data not shown).

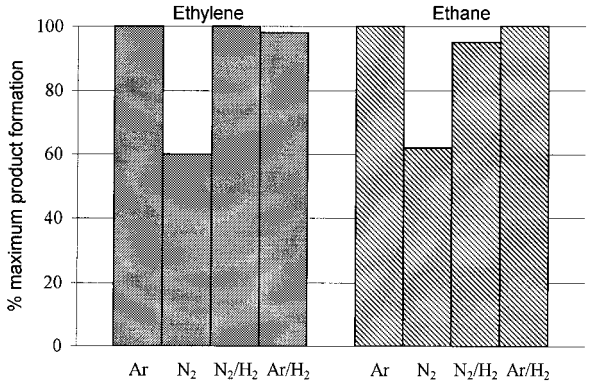

FIGURE 5: Inhibition by N_2 of C_2H_2 reduction to both C_2H_4 and C_2H_6 by the α-195^{Asn} MoFe protein and the effect of added H_2. Assays were conducted under 1 kPa C_2H_2 with either 100 kPa Ar or 100 kPa N_2. H_2, when present, was at an additional 101 kPa, resulting in a total of 202 kPa (2 atm). Maximum C_2H_4 and C_2H_6 production was 184 and 58 nmol per assay, respectively.

Table 2: Summary of the Pertinent Catalytic Properties of Wild-Type and Altered MoFe Proteins

	properties					
	with dinitrogen				with azide	
MoFe protein	binding	reduction rate	H_2 inhibition	HD formation	rate[a]	flux inhibition[b]
wild type	yes	high	yes	yes	high	no
α-195^{Gln} [c]	yes	very low	yes	yes	low	yes; ≈65%
α-195^{Asn}	yes	zero	yes	no	low	yes; ≈20%
α-191^{Lys}	no	zero	N/A[d]	N/A[d]	low	no

[a] Based on the rates of N_2H_4 and NH_3 formation from 10 mM sodium azide. [b] Relative to each MoFe protein's rate of H_2 evolution under 101 kPa argon. Based on the assumption that the N_2-production rate from 10 mM sodium azide could equal but not exceed the rate of NH_3 production. [c] All data for the α-195^{Gln} MoFe protein are taken from ref *29*. [d] N/A: with no N_2 binding observed, the H_2-inhibition and HD-formation reactions are moot.

Azide (at 10 mM) inhibited electron flux through the α-195^{Asn} MoFe protein by ca. 20%, which was much less than the ca. 65% inhibition observed with the α-195^{Gln} MoFe protein. In contrast, azide inhibition of electron flux was negligible for both the wild-type and α-191^{Lys} MoFe proteins. Also, because the rate of MgATP hydrolysis was not inhibited by added azide, the inhibition of electron flux to products, where it occurred, resulted in a proportional increase in the ATP/2e^- ratio.

Table 2 summarizes the pertinent properties of the wild-type and the altered α-195^{Asn}, α-195^{Gln}, and α-191^{Lys} MoFe proteins.

DISCUSSION

Although both the α-195^{Asn} and α-191^{Lys} MoFe proteins are incapable of catalyzing the reduction of N_2, their rates

of H_2 evolution responded differently when assayed under a N_2 atmosphere rather than the normal Ar atmosphere. The H_2-evolution rate of the α-191^{Lys} MoFe protein was unchanged, whereas the H_2-evolution rate of the α-195^{Asn} MoFe protein was decreased relative to the rate under Ar. A similar effect was observed when N_2 was introduced into C_2H_2-reduction assays, where again only the α-195^{Asn} MoFe protein showed a clear (and identical) decrease in the rates of both C_2H_4 and C_2H_6 production. However, the inhibition by N_2 is easily observed only at a low partial pressure of C_2H_2, explaining why it was not noted earlier. Clearly, N_2 interacts with the α-195^{Asn} MoFe protein, even though, unlike the α-195^{Gln} MoFe protein (*29*), N_2 is not a substrate for the α-195^{Asn} MoFe protein. N_2 appears to behave as a reversible "competitive" inhibitor of electron flux through the α-195^{Asn} MoFe protein as observed with the α-195^{Gln} MoFe protein (*34*). Moreover, N_2 appears to do so through binding at its normal reduction site because added H_2 relieved the N_2 inhibition of C_2H_2 reduction and H_2 is a well-known, specific inhibitor of N_2 binding and reduction by wild-type Mo-nitrogenase.

This last result led us to expect that HD would be produced, as found with the α-195^{Gln} MoFe protein (*29, 48*), when the α-195^{Asn} MoFe protein was turned over under a 1:1 D_2/N_2 atmosphere. All evidence presented so far suggests that H_2 inhibition of N_2 binding (and reduction, where it occurs) and HD formation under a D_2/N_2 atmosphere are manifestations of the same molecular process (see the introduction). However, quite surprisingly, no HD was formed under these conditions with the α-195^{Asn} MoFe protein. The only observable effect of the added D_2 was relief of the N_2-induced inhibition of electron flux. This result is the first observation to indicate that H_2 (and, of course, D_2) inhibition of N_2 binding is not the result of exactly the same reaction that leads to HD formation under a D_2/N_2 atmosphere.

How is it possible to separate these two reactions? Obviously, both H_2 and D_2 must be capable of performing exactly the same chemistry on nitrogenase. The only reason for using D_2 is simply one of detection. So, if H_2 and D_2 are not the source of discrimination between the H_2 (and D_2) inhibition of N_2 binding and HD formation under D_2/N_2, then the source must reside on the α-195^{Asn} MoFe protein itself. Our preferred explanation is based on the inability of the α-195^{Asn} MoFe protein to reduce N_2 to NH_3. This inability is a major difference between the α-195^{Asn} MoFe protein and both the wild-type and α-195^{Gln} MoFe proteins, both of which catalyze N_2 reduction to NH_3, albeit at vastly different rates, and produce HD under N_2/D_2. This difference may be the source of the discrimination by the α-195^{Asn} MoFe protein between the H_2-inhibition and HD-formation reactions. In the Lowe−Thorneley scheme, N_2 *binds* at the E_3 redox level and suffers competition from H_2 (and D_2) at this level, but *reduction* of N_2 (as shown, e.g., by the recovery of N_2H_4 on quenching; *15*) may occur only after the E_4 redox level is attained. Thus, the ability to *bind* N_2 may simply not be sufficient for HD formation, which may require a *reduced* form of N_2. Therefore, the α-195^{Asn} MoFe protein may be incapable of reaching the E_4 redox level and so is incapable of catalyzing both the N_2-reduction and HD-formation reactions. A logical extension of this explanation is that the α-191^{Lys} MoFe protein cannot bind N_2 because it is incapable of achieving even the E_3 redox level.

This explanation for the dichotomy between the H_2-inhibition reaction and the HD-formation reaction re-opens the question of the nature of the required reduced-nitrogen intermediate. An earlier model suggested that a two-electron-reduced, enzyme-bound, diazene-level (N_2H_2) intermediate could be decomposed by D_2 to produce two HD molecules and release N_2 intact (*22, 23*). This reaction accounts for both the stoichiometry of only one electron being required for each HD molecule formed and the observation that a small amount of N_2 is capable of producing a considerable quantity of HD (*22*). The latter property of this model might also account for the wild-type rate of HD formation from the α-195^{Gln} MoFe protein despite its very low rate of NH_3 production (*29*). In fact, the wide discrepancy in these two rates led us to suggest earlier that a reduced N−N intermediate might not be involved in HD formation. Now it appears that only a small fraction of the MoFe protein carrying a reduced N−N species could be sufficient for substantial HD formation under N_2.

At the time that this model was proposed, the H_2-inhibition reaction and the HD-formation reaction were thought to be consequences of the same nitrogenase chemistry, so that the model suffered the shortcoming of being incompatible with the known competitive inhibition by H_2 (or D_2) of N_2 reduction (*25*). Interception of an enzyme-bound reduced N−N intermediate by D_2 (or H_2) would predict a noncompetitive kinetic pattern. Now, our current data indicate that this objection may no longer be valid and HD formation under N_2/D_2 could involve a partially reduced (and probably partially protonated) N−N species. However, although the enzyme apparently needs to be at the [E_4] redox level, it remains to be determined whether the reduced N−N species is at the diazene level, the hydrazine level, or some other level of reduction.

An alternative explanation, which does not depend on the reduction of N_2, is based on the chemistry of Mo−N_2 and Mo−hydride complexes (*49*), where evolution of H_2 occurs *after* N_2 is bound. In these complexes then (and possibly with nitrogenase), H_2 evolution is not necessary to generate a N_2 binding site but may be a consequence of having to protonate the metal center before it can accept electrons. Moreover, the extent of labilization of these hydrides on a metal center, e.g., $MoH_2(N_2)$, may depend on the strength of the metal−N_2 interaction. Thus, when the Mo−N_2 interaction is strong, the Mo−H bonds will be more susceptible to protonation and vice versa. If simultaneous binding of N_2 and hydrides to nitrogenase occurs, then the hydrides on those enzymes, which are capable of reducing N_2, should be more labile than the hydrides on the non-N_2-reducing enzymes, assuming that higher N_2-reduction rates indicate a stronger interaction of N_2 with the enzyme. Thus, when deuterides are present, e.g., E−$D_2(N_2)$, the extent to which they are activated toward protonation to give HD would again depend on the strength of the E−(N_2) interaction. Our data are consistent with this hypothesis because it is those enzymes, which reduce N_2 to NH_3, that also produce HD. A drawback with this hypothesis, however, is that it does not easily accommodate the separation of the H_2-inhibition reaction from the HD-forming reaction.

These new insights into N_2-based reactions led us to probe azide reduction from which N_2 is produced via reaction 4 below. If nitrogenase catalyzes only reactions 3−5 below

(*39, 40*), then, because neither the α-195^{Asn} nor the α-191^{Lys} MoFe protein reduces N_2, i.e., reaction 5 is inoperative, the rate of N_2 production from azide by the α-195^{Asn} and α-191^{Lys} MoFe proteins could be calculated as the difference between the measured rates of NH_3 and N_2H_4 production:

$$HN_3 + 6e^- \rightarrow N_2H_4 + NH_3 \quad (3)$$

$$N_3^- + 2e^- \rightarrow N_2 + NH_3 \quad (4)$$

$$N_2 + 6e^- \rightarrow 2NH_3 \quad (5)$$

In fact, reaction 5 has been offered as a rationale for wild-type nitrogenase's production of "excess NH_3", that is, NH_3 produced over and above the combined amounts of N_2 and N_2H_4 (*39*−*41*). Based on the effects of adding D_2 to azide-reducing assays, N_2 was proposed as a likely reactive intermediate because the rate of N_2 production was increased whereas the rate of "excess NH_3" production was concomitantly decreased with no effect on the rate of H_2 evolution. This result is exactly what would be expected if the added D_2 was inhibiting reaction 5 by diverting electron flux to HD formation (*40*), but HD formation was not measured. When we performed similar experiments with either wild type or the α-195^{Gln} MoFe protein (*29*), no HD was formed. Also in those same experiments with the α-195^{Gln} MoFe protein (*29*), D_2 had no significant effect on the rates of both N_2 and NH_3 production from azide, even though added H_2 had completely eliminated NH_3 production from N_2 with this same altered MoFe protein. Moreover, in the present work, added H_2 again had no effect on the rates of both N_2 and NH_3 production from azide reduction catalyzed by the α-195^{Asn} MoFe protein. Thus, if the N_2 produced from azide reduction is the source of "excess NH_3" via reaction 5, it is apparently not undergoing the same chemistry, at least not on these altered MoFe proteins, as that which occurs when N_2 is present as the only substrate. An alternative explanation is that "excess NH_3" may be produced by a direct eight-electron reduction of azide without the intermediacy of N_2 as has been suggested previously (*39*) and as shown in reaction 6. If reaction 6 does function during azide reduction catalyzed by these altered MoFe proteins, our simple assumption for calculating the rate of N_2 production as the difference between the rates of NH_3 and N_2H_4 production is invalidated.

$$N_3^- + 8e^- \rightarrow 3NH_3 \quad (6)$$

We could, however, make the alternative assumption that N_2 and N_2H_4 are produced from azide in a constant molar ratio (ca. 4:1, see Table 1). Then, we find that the α-195^{Asn} MoFe protein likely produces "excess NH_3" and so may utilize reaction 6, but the α-191^{Lys} MoFe protein does not. This difference may reflect the generally poorer catalytic capacity of the α-191^{Lys} MoFe protein.

We found that azide induced the inhibition of electron flux to products with both the α-195^{Asn} and α-195^{Gln} MoFe proteins. N_2 is unlikely to be responsible for this azide-induced inhibition of electron flux to products because the wild-type MoFe protein produces more N_2 than the α-195^{Gln} MoFe protein but suffers effectively no electron-flux inhibition. The variation in the extent of electron-flux inhibition by azide that is observed with these altered MoFe proteins, all of which maintain the ability to reduce azide to a similar extent (although poorly), suggests that N_3^- has two binding sites. The first site acts as a substrate-binding and -reduction site, whereas the second site is an electron-flux inhibition site. This situation parallels the two sites indicated for C_2H_4 (and, possibly, C_2H_2) binding (*37, 50*). However, it is unlikely that both N_3^- and C_2H_4 use the same flux-inhibition site because electron-flux inhibition by C_2H_4 cannot be fully relieved by added CO (*37, 50*), whereas that due to N_3^- binding is fully relieved by CO (*29*). A possible alternative is that only a single azide-binding site exists. If so, a better comparison might be with the substrate/inhibitor (HCN/CN^-) pair supplied by sodium cyanide solutions (*38, 51*−*52*), where CO does fully relieve electron-flux inhibition by CN^-. Here, CN^- binds to the wild-type enzyme and acts as an electron-flux inhibitor until it is protonated to give the substrate (either HCN or HNC), which is then reduced (*52*).

The results from previous studies of the interactions of either cyanide or azide with nitrogenase (*38, 40, 51*), under higher-flux conditions, provide some support for our suggestion. First, both of the uncharged substrates, HCN and HN_3, apparently bind to, and are reduced by six electrons at, redox states of the wild-type enzyme more oxidized than those required to either reduce N_2 or evolve H_2, which at high electron flux are [E_3] and [E_4]. Second, azide interferes with (and partially relieves) the electron-flux inhibition caused by CN^-. Both similarities indicate common interactions with the enzyme. A major difference is that the anionic species, N_3^-, is a substrate for the wild-type nitrogenase, not an electron-flux inhibitor as is the case for CN^-. This property of N_3^- may not negate our argument, however, because N_3^- is an electron-flux inhibitor as well as a presumed substrate (as indicated by NH_3 being produced in considerable excess over N_2H_4; see reactions 3 and 4 above) with both the α-195^{Asn} and α-195^{Gln} MoFe proteins (*29*). Moreover, CN^- is not an electron-flux inhibitor with the α-195^{Gln} MoFe protein (*29*). These observations indicate that quite conservative changes in the FeMo-cofactor environment can result in substantial changes in the reactivity of bound substrates/inhibitors.

The last thought leads to the question as to whether the observed reactivity changes can be correlated with any structural change caused by substituting the α-195^{His} residue. The amide N of a substituting glutamine residue can be disposed similarly to the imidazole ϵ-N of histidine with respect to the FeMo-cofactor surface (because the chain length from the backbone α-carbon to either nitrogen is the same), but the amide N of an asparagine cannot (*34*). Thus, the NH→S hydrogen bonding to one of the central S atoms in the wild-type MoFe protein (*2, 3*) is likely to be maintained in the α-195^{Gln} MoFe protein but disrupted in the α-195^{Asn} MoFe protein. This difference could result in localized effects on the electronic structure of the FeMo-cofactor. Support for this suggestion is found in the corresponding EPR signals of the two altered MoFe proteins (*35*). Even so, the presence of the putative α-195^{Gln} NH→S hydrogen bond is clearly inadequate for normal rates of N_2 reduction. However, the NH→S hydrogen bond has a role to play because in its absence, as exemplified by the α-195^{Asn} substitution, N_2 is not reduced although it still binds.

An attractive thought is that the α-195^{His} residue is involved in proton transfer during substrate reduction (*38*). If so, the very different pK_a of an imidazole N−H compared to that of an amide N−H could contribute to the different reactivity toward N_2. Further, the presence or absence of an NH→S hydrogen bond, which could affect the pK_a of the involved group, could explain the difference in reactivity of the α-195^{Gln} MoFe protein compared with the α-195^{Asn} MoFe protein. If the α-195^{His}-based NH→S hydrogen bond is required for effective protonation of N_2, it is clearly not necessary for proton delivery to azide. It may still be the preferred proton donor, but, because the α-195^{Asn} MoFe protein is a somewhat more effective catalyst for azide reduction than the α-195^{Gln} MoFe protein, alternative proton-donor source(s) are likely available to this substrate. One alternative proton donor may involve the α-191^{Gln} residue and its interaction with homocitrate, as proposed for the HCN/CN^- system (*38*). The presence of alternative proton donors would help explain the comparable rates of azide reduction exhibited by both the α-195^{Asn} and α-191^{Lys} MoFe proteins.

ACKNOWLEDGMENT

All mutant strains used in this study were constructed in an earlier collaborative project with D. R. Dean (Virginia Tech).

REFERENCES

1. Bulen, W. A., and LeComte, J. R. (1966) *Proc. Natl. Acad. Sci. U.S.A. 56*, 979−986.
2. Kim, J., and Rees, D. C. (1992) *Science 257*, 1677−1682.
3. Kim, J., and Rees, D. C. (1992) *Nature 360*, 553−560.
4. Peters, J. W., Stowell, M. H. B., Soltis, S. M., Finnegan, M. G., Johnson, M. K., and Rees, D. C. (1997) *Biochemistry 36*, 1181−1187.
5. Schindelin, H., Kisker, C., Schlessman, J. L., Howard, J. B. and Rees, D. C. (1997) *Nature 387*, 370−376.
6. Shah, V. K., and Brill, W. J. (1977) *Proc. Natl. Acad. Sci. U.S.A. 78*, 3249−3253.
7. Hawkes, T. R., McLean, P. A., and Smith, B. E. (1984) *Biochem. J. 217*, 317−321.
8. Scott, D. J., May, H. D., Newton, W. E., Brigle, K. E., and Dean, D. R. (1990) *Nature 343*, 188−190.
9. Bulen, W. A., Burns, R. C., and LeComte, J. R. (1965) *Proc. Natl. Acad. Sci. U.S.A. 53*, 532−539.
10. May, H. D., Dean, D. R., and Newton, W. E. (1991) *Biochem. J. 277*, 457−464.
11. Peters, J. W., Fisher, K., Newton, W. E. and Dean, D. R. (1995) *J. Biol. Chem. 270*, 27007−27013.
12. Lanzilotta, W. N., and Seefeldt, L. C. (1996) *Biochemistry 35*, 16770−16776.
13. Erickson, J. A., Nyborg, A. C., Johnson, J. L., Truscott, S. M., Gunn, A., Nordmeyer, F. R., and Watt, G. D. (1999) *Biochemistry 38*, 14279−14285.
14. Hageman, R. V., and Burris, R. H. (1978) *Proc. Natl. Acad. Sci. U.S.A. 75*, 2699−2702.
15. Lowe, D. J., and Thorneley, R. N. F. (1984) *Biochem. J. 224*, 877−909.
16. Thorneley, R. N. F., and Lowe, D. J. (1985) in *Molybdenum Enzymes* (Spiro, T. G., Ed.) pp 222−284, Wiley, New York.
17. Fisher, K., Lowe, D. J., and Thorneley, R. N. F. (1991) *Biochem. J. 279*, 81−85.
18. Lowe, D. J., Fisher, K., and Thorneley, R. N. F. (1990) *Biochem. J. 272*, 621−625.
19. Strandberg, G. W., and Wilson, P. W. (1968) *Can. J. Microbiol. 14*, 25−31.
20. Hadfield, K. L., and Bulen, W. A. (1969) *Biochemistry 8*, 5103−5108.
21. Hwang, J. C., Chen, C. H., and Burris, R. H. (1973) *Biochim. Biophys. Acta 292*, 256−270.
22. Burgess, B. K., Wherland, S., Newton, W. E., and Stiefel, E. I. (1981) *Biochemistry 20*, 5140−5146.
23. Hoch, G. E., Schneider, K. C., and Burris, R. H. (1960) *Biochim. Biophys. Acta 292*, 256−270.
24. Jackson, E. K., Parshall, G. W., and Hardy, R. W. F. (1968) *J. Biol. Chem. 243*, 4952−4958.
25. Guth, J. H., and Burris, R. H. (1983) *Biochemistry 22*, 5111−5122.
26. Li, J.-H., and Burris, R. H. (1983) *Biochemistry 22*, 4472−4480.
27. Burgess, B. K., Corbin, J. L., Rubinson, J. F., Li, J.-G., Dilworth, M. J., and Newton, W. E. (1984) in *Advances in Nitrogen Fixation Research* (Veeger, C., and Newton, W. E., Eds.) p 146, Nijhoff-Junk, The Hague.
28. Jensen, B. B., and Burris, R. H. (1985) *Biochemistry 24*, 1141−1147.
29. Dilworth, M. J., Fisher, K., Kim, C.-H., and Newton, W. E. (1998) *Biochemistry 37*, 17495−17505.
30. Wherland, S., Burgess, B. K., Stiefel, E. I., and Newton, W. E. (1981) *Biochemistry 20*, 5132−5140.
31. Burgess, B. K., and Lowe, D. J. (1996) *Chem. Rev. 96*, 2983−3011.
32. Newton, W. E., Bulen, W. A., Hadfield, K. L., Stiefel, E. I., and Watt, G. D. (1977) in *Recent Developments in Nitrogen Fixation* (Newton, W., Postgate, J. R., and Rodriguez-Barrueco, C., Eds.) pp 119−130, Academic Press, London.
33. Scott, D. J., Dean, D. R., and Newton, W. E. (1992) *J. Biol. Chem. 267*, 20002−20010.
34. Kim, C.-H., Newton, W. E., and Dean, D. R. (1995) *Biochemistry 34*, 2798−2808.
35. DeRose, V. J., Kim, C.-H., Newton, W. E., Dean, D. R., and Hoffman, B. M. (1995) *Biochemistry 34*, 2809−2814.
36. Shen, J., Dean, D. R., and Newton, W. E. (1997) *Biochemistry 36*, 4884−4894.
37. Fisher, K., Dilworth, M. J., Kim, C.-H., and Newton, W. E. (2000) *Biochemistry 39*, 2970−2979.
38. Fisher, K., Dilworth, M. J., Kim, C.-H., and Newton, W. E. (2000) *Biochemistry 39*, 10855−10865.
39. Dilworth, M. J., and Thorneley, R. N. F. (1981) *Biochem. J. 193*, 971−983.
40. Rubinson, J. F., Burgess, B. K., Corbin, J. L., and Dilworth, M. J. (1985) *Biochemistry 24*, 273−283.
41. Hardy, R. W. F., and Knight, E., Jr. (1967) *Biochim. Biophys. Acta 139*, 69−90.
42. Lowry, O. H, Rosebrough, N. J., Farr, A. L., and Randall, R. J. (1951) *J. Biol. Chem. 193*, 265−275.
43. Dilworth, M. J., Eldridge, M. E., and Eady, R. R. (1992) *Anal. Biochem. 207*, 6−10.
44. Dilworth, M. J., and Fisher, K. (1998) *Anal. Biochem. 256*, 242−244.
45. Ennor, A. H. (1957) *Methods Enzymol. 3*, 850−856.
46. Rivera-Ortiz, J. M., and Burris, R. H. (1975) *J. Bacteriol. 123*, 537−545.
47. Davis, L. C., and Wang, Y.-L. (1980) *J. Bacteriol. 3*, 1230−1238.
48. Kim, C.-H. (1994) Ph.D. Thesis, Virginia Tech, Blacksburg, VA.
49. Hughes, D. L., Ibrahim, S. K., Pickett, C. J., Querne, G., Laouenan, A., Talarmin, J., Queiros, A., and Fonseca, A. (1994) *Polyhedron 13*, 3341−3348.
50. Ashby, G. A., Dilworth, M. J., and Thorneley, R. N. F. (1987) *Biochem. J. 247*, 547−554.
51. Li, J.-G., Burgess, B. K., and Corbin, J. L. (1982) *Biochemistry 21*, 4393−4402.
52. Lowe, D. J., Fisher, K., Thorneley, R. N. F., Vaughn, S. A., and Burgess, B. K. (1989) *Biochemistry 28*, 8460−8466.
53. Kraulis, P. (1991) *J. Appl. Crystallogr. 24*, 946−950.

BI0017834